J. Phys. B: Atom. Molec. Phys., 1971, Vol. 4. Printed in Great Britain

Measurement of the cross sections for electron impact ionization of multi-electron ions I. O^+ to O^{2+} and O^{2+} to O^{3+}

K. L. AITKEN and M. F. A. HARRISON

United Kingdom Atomic Energy Authority, Culham Laboratory, Abingdon, Berkshire

MS. received 22nd April 1971

Abstract. The technique of crossed electron–ion beams has been used to make absolute measurements of the electron impact ionization cross section for the reaction $O^+ + e \rightarrow O^{2+} + 2e$. Incident electron energies ranged from below threshold up to 1000 eV and at energies above 100 eV the cross section can be expressed as,

$$Q = \frac{1530}{E} \lg \frac{E}{55{\cdot}0} \ (10^{-17} \text{ cm}^2)$$

where E is the electron impact energy in eV. A similar measurement for $O^{2+} + e \rightarrow O^{3+} + 2e$ up to an incident energy of 500 eV yields the expression

$$Q = \frac{626}{E} \lg \frac{E}{55{\cdot}0} \ (10^{-17} \text{ cm}^2).$$

Evidence for the presence of metastable oxygen ions in the parent ion beams is presented and their influence on the measured cross sections discussed. The experimental results are compared with a Coulomb–Born calculation by Moores, a classical binary encounter calculation by Thomas and Garcia, and a semiempirical estimate by Lotz. Comparison of the present measurements for O^+ with the ionization cross section of the isoelectronic nitrogen atom supports the measurements of Smith *et al.* for this atom. A comparison is also made between O^{2+} and its isoelectronic ion N^+.

1. Introduction

Electron impact ionization processes involving multi-electron ions are of importance to astrophysics, atmospheric physics and the study of electrical discharges. In particular the presence of such ions in the hydrogen ion plasmas of fusion confinement devices causes enhanced losses of energy due to bremsstrahlung radiation and of hydrogen atoms due to charge exchange.

In the case of atmospheric ions, there have been no previous experimental measurements of ionization cross sections with the exception of that for N^+ to N^{2+} by Harrison *et al.* (1963). Theoretical determinations have for the most part been restricted to classical binary encounter methods (for example, Thomas and Garcia 1969) or to semiempirical methods such as that of Lotz (1968). The only calculations using quantum theory have been those of D. L. Moores (1970, private communication) who has applied the Coulomb–Born approximation. The lack of experimental data to support theory, which is of questionable accuracy in the case of such complex ions, has provided a strong incentive for the present series of investigations.

A. $O^+ + e \rightarrow O^{2+} + 2e$

2. Apparatus and method

The experimental approach was that of crossed electron and ion beams and the

apparatus, which is shown schematically in figure 1, was similar to that used by Dance *et al.* (1967a). Oxygen ions were formed by electron bombardment in a P.I.G. type ion source. To reduce erosion of the heated tungsten filament, the source was fed with a 3 to 1 mixture of He and O_2 at a total pressure not exceeding 5×10^{-3} torr and the discharge current was maintained at the low value of 8 mA. Ions were extracted

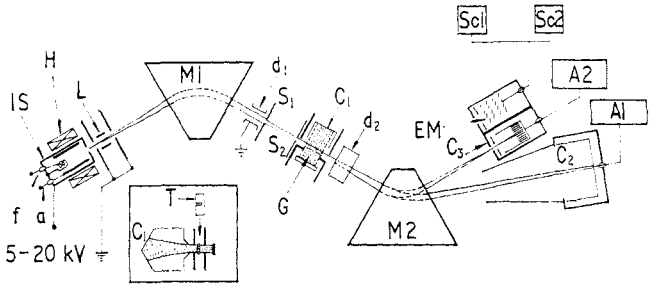

Figure 1. Schematic view of the apparatus. IS, ion source, with anode a, filament f, and axial magnetic field windings H; L, einzel lens; M1, selector magnet and M2, analyser magnet; d_1 and d_2 are respectively ion beam pulsing and vertical deflector plates; S_1 and S_2, collimating slits; G, electron gun with collector C_1, and slotted shutter T (see inset); C_2, Faraday cup with dc amplifier A1, for parent ion beam; C_3, Faraday cup with Cary 401 electrometer A2, for product ion; EM, model MM1 Johnston electron multiplier for single-particle counting of product ions using gated synchronized scalers Sc 1, and Sc 2.

through a potential difference of 15 kV. A beam of O^+ (charge to mass ratio = 16) was selected by the first magnetic field and collimated by apertures before passing through the electron beam. Product ions of O^{2+} were separated from the parent ion beam leaving the collision region by a second magnetic field and were detected by a Johnston Laboratories MM1 electron multiplier. The multiplier which had an efficiency of 100 $(+0, -2{\cdot}5)\%$ was mounted together with a Faraday cup in the manner described by Dance *et al.* (1967b). It was calibrated by comparing the count rate for a weak beam of O^{2+} ions extracted from the source (extraction potential, 7·5 kV) with the corresponding ion current collected in the cup and measured by a Cary Model 401 electrometer.

The flux of product ions from electron ionization was superimposed upon a background of O^{2+} ions which was typically 15 times greater. These ions were attributed to charge stripping of the parent beam on surfaces and residual gas, even though the pressure in the collision region did not exceed 2×10^{-9} torr. The signal was isolated from this background by pulsing both beams and using synchronized gated scalers (Harrison 1968). Typical operating conditions were: signal, 1500 counts per sec.; instantaneous pulsed current of O^+ ions, $3{\cdot}0 \times 10^{-8}$ A; and instantaneous pulsed current of electrons, 1·0 mA.

Since the beams cross at right angles and all the electrons pass completely through the ion beam, the cross section can be expressed in terms of the experimental parameters by

$$Q(E) = \frac{RN}{IJ} \frac{vV}{(v^2+V^2)^{1/2}} e^2 hF \frac{1}{\Omega}. \tag{1}$$

In this equation E is the incident electron energy given by $E = \frac{1}{2}m_e(v^2+V^2)$ where v, V are respectively the electron and ion velocities. R is the signal count rate corrected

for electronic dead time and Ω the detector efficiency. The electron and ion beam instantaneous currents are J and I and the charge of the parent ion is Ne. The height of the ion beam in the collision region is h and F is a beam overlap factor ($> 0{\cdot}99$) measured using the scanning shutter shown in figure 1.

At most incident electron energies the signal was shown to be proportional to electron current. The maximum acceptable electron current varied from 60 μA at low energies to about 1·2 mA at higher energies. A few measurements were made at single electron currents which were well within the linear regime. The incident electron energy was calibrated by observing the onset of production of Ne^{2+} from a parent beam of Ne^{+} and a correction, attributed to contact potentials and field penetration into the collision region, of $-2{\cdot}5 \pm 0{\cdot}5$ eV was applied at all energies. Previous retarding potential measurements showed that 90% of the electrons were within $\pm 1{\cdot}5$ eV of the mean energy.

3. Molecular ions in the parent beam

Atomic ion beams extracted from discharges in diatomic molecular gases are likely to be contaminated by molecular ions. In the present experiment O_2^{2+} ions (charge to mass ratio = 16) cannot be separated from parent O^{+} ions and can give rise to O^{2+} ions by the following dissociation reaction,

$$O_2^{2+} + e \rightarrow O^{2+} + O + e.$$

The threshold energy for this reaction is likely to lie below that for ionization of O^{+} and thus dissociation should manifest itself by an apparent cross section which does not fall to zero at the ionization threshold. Fortunately the relatively high threshold energy for the production of O_2^{2+} by direct electron impact in the ion source (Dorman and Morrison 1963) indicates that the population of molecular ions should be sensitive to the potential applied to the anode in the P.I.G. source and could be negligible at low potentials. Further, there is some direct evidence (Harrison *et al.* 1963) that such dissociation cross sections are likely to fall rapidly with energy and could be small at energies above the threshold for ionization of O^{+}.

Evidence of the presence of O_2^{2+} was obtained by measuring the apparent cross section Q_a at energies below the threshold of O^{+}. The results are shown in figure 2 for two different potentials (75 V and 150 V) applied to the anode of the ion source. At the higher anode potential the apparent cross section shows an appreciable signal below threshold which falls rapidly with increasing energy until at energies somewhat in excess of threshold the apparent cross section becomes insensitive to anode potential. At incident energies above 25 eV the difference between the two apparent cross sections exhibits an E^{-3} dependence upon energy which is not incompatible with molecular dissociation. Further support for the presence of O_2^{2+} at the 150 V condition is provided by the magnitude of the background of O^{2+} ions which was about 2·5 times greater than for the 75 V condition; the increase being attributed to dissociation of O_2^{2+} on gas and surfaces. Observation of the $(O_{16}O_{17})^{2+}$ peak under the 150 V condition was masked by overlapping peaks but demonstrated that the concentration of O_2^{2+} was not greater than 2%.

The ratios of O^{2+} to O^{+} ion yields from the source were about 1% and 0·1% at 150 V and 75 V respectively; thereby indicating that a significant number of O_2^{2+} ions was unlikely to be present at the lower potential. This conclusion is substantiated by the fact that Q_a measured under the 75 V condition exhibits an $E^{-1/2}$ energy

dependence below the O^+ ionization threshold and has negative values. This behaviour is typical of an ion beam without dissociating components and arises from changes in ion collection efficiency caused by deflection of ion trajectories by space charge of the electron beam (Harrison 1968).

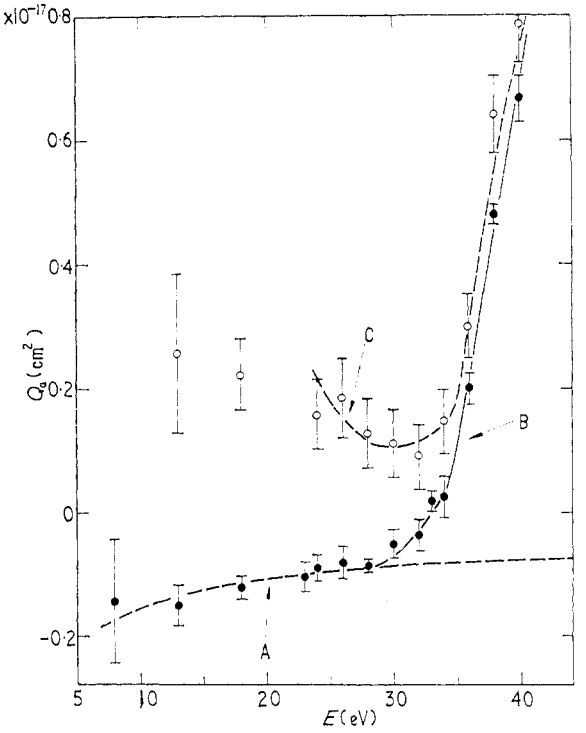

Figure 2. Apparent cross section as a function of incident electron energy for different potentials applied to the anode of the ion source, ● 75 V and ○ 150 V. Curve A is the signal below threshold for the 75 V condition expressed as a function of $E^{-1/2}$ and curve B is drawn smoothly through the experimental points. Curve C is the difference between the apparent cross sections for these two conditions expressed as a function of E^{-3} and plotted relative to curve B. Error bars represent 90% limits of random errors.

Data at the 150 V potential was thus corrected using an E^{-3} term determined from the below threshold signal and combined with that obtained at the 75 V potential. The combined data was further corrected using an $E^{-1/2}$ term, similarly determined, to yield the measured ionization cross section. The correction amounts to less than 1% at the peak value of the measured cross section.

4. Metastable O^+ ions in the parent beam

The measured cross section $Q(E)$ is plotted against incident electron energies up to 50 eV in figure 3. The onset of ionization occurs below the $^4S^0$ ground state threshold and shows that metastable ions were present in the parent beam. Daly and Powell (1967) and Redhead (1969) have studied the onset of ionization from O^+ ions and observed ionization from the $^2P^0$ and $^2D^0$ metastable states whose lifetime (Bates 1960) are 3·6 h and 5 s respectively. Ionization channels likely to be

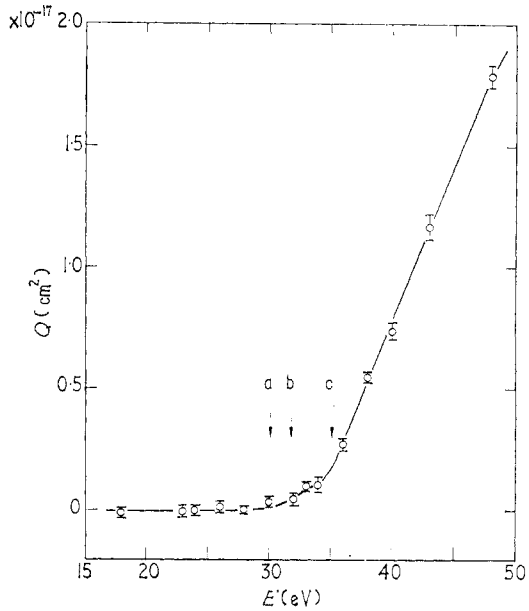

Figure 3. Measured cross section of O^+ as a function of incident electron energy close to threshold. Error bars show the 90% confidence limits of the random errors. The arrows a, b and c show respectively the threshold energies for the $^2P^0$, $^2D^0$ metastable states and the $^4S^0$ ground state.

of significance in the present experiment are:

Outer shell ionization

$$O^+(1s^22s^22p^3)\begin{cases}\longrightarrow {}^2P^0\ (30{\cdot}1\text{ eV})\\ \longrightarrow {}^2D^0\ (31{\cdot}8\text{ eV})\\ \longrightarrow {}^4S^0\ (35{\cdot}1\text{ eV})\end{cases}\longrightarrow O^{2+}(1s^22s^22p^2)$$

Inner shell ionization

$$O^+(1s^22s^22p^3)\begin{cases}\longrightarrow {}^2P^0\ (37{\cdot}6\text{ eV})\\ \longrightarrow {}^2D^0\ (39{\cdot}3\text{ eV})\\ \longrightarrow {}^4S^0\ (42{\cdot}6\text{ eV})\end{cases}\longrightarrow O^{2+}(1s^22s2p^3)$$

Statistical uncertainties in the signal combined with spread in the electron beam energy preclude identification of the separate contributions of the $^2P^0$ and $^2D^0$ states to outer shell ionization. Similarly it is not possible to identify positively any of the inner shell contributions.

Since the experiment cannot resolve between ionization from the $^2P^0$ and $^2D^0$ states, the measured cross section can be expressed as

$$Q(E) = fQ_m(E) + (1-f)Q_g(E) \tag{2}$$

where f is the total fractional concentration of both metastable states, $Q_m(E)$ is an

ionization cross section averaged over both states and $Q_g(E)$ the ionization cross section for the ground state. The data below and immediately above ground state threshold shows a linear dependence upon energy, so that in this restricted energy range the ratio of these slopes, S_m and S_t respectively, is given by:

$$\frac{S_m}{S_t} = \frac{fQ_m}{fQ_m + (1-f)Q_g}. \tag{3}$$

Hence

$$f = \frac{S_m K}{S_t - S_m(1-K)} \tag{4}$$

where $K = Q_g/Q_m$. The cross sections for ionization of the $^2P^0$ and $^2D^0$ states were calculated using the Lotz formulation and the value of their ratio K found to be 0·794 at the peaks of the cross sections. As a crude approximation, K calculated at the peak of the cross section is assumed to be valid near threshold and together with the calculated value of Q_m yields a total fractional concentration of metastable ions of 20·0 $(-3·0, +8·0)\%$. Here the errors are assessed from uncertainties both in determining the slopes and in averaging Q_m, the latter being due to the unknown relative population of the two metastable states. The results are in reasonable agreement with an independent determination by Turner *et al.* (1968) although these authors found

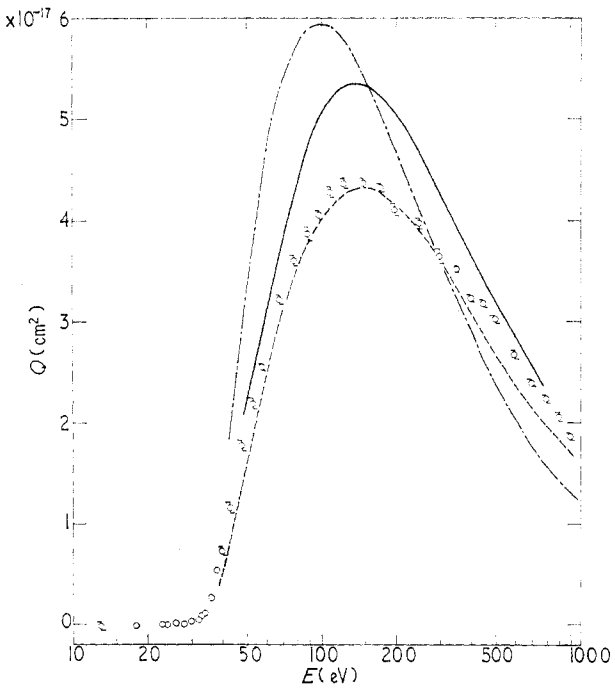

Figure 4. Measured cross section of O^+ as a function of incident electron energy up to the limit of experiment at 1 keV. The solid line shows the Coulomb–Born approximation of Moores (1970 private communication), the dashed line shows the semiempirical formulation of Lotz (1968) and the broken line the classical binary encounter calculation of Thomas and Garcia (1969). Experimental points are shown with open circles and have error bars giving the 90% confidence limits where these exceed the circle diameters.

evidence that the metastable yield from their electron bombardment ion source contained only the $^2D^0$ state. As a diagnostic test, the present source was fed with pure O_2 gas but no significant change was observed in the yields of either O_2^{2+} or metastable O^+ and it is concluded that the normal presence of He gas in the source did not influence the contribution from these extraneous ions.

Substitution for f in equation (2) and using the Lotz values for Q_m and Q_g indicates that the measured cross section is likely to overestimate the ground state cross section by not more than 6·0% at the peak, falling to 4·5% at 500 eV.

5. Results and discussion

The measured cross section is shown as a function of incident energy in figure 4, where the bars represent 90% confidence limits of the random errors. The data is also presented numerically in table 1 together with the maximum possible values of

Table 1. Electron impact ionization of O^+ to O^{2+}

Mean incident electron energy† (eV)	Measured cross section (10^{-17} cm^2)	Random error‡ ± %	Maximum possible systematic error (%)¶
28	0·005	130	±180
30	0·034	65	+32 −30·0
32	0·045	46	+25·0 −23·0
33	0·098	15	+15·0 −13·0
34	0·107	27	+14·5 −12·5
36	0·270	9	+10·0 − 8·0
38	0·545	3	+ 9·0 − 7·0
40	0·736	5	+ 8·0 − 6·0
43	1·17	4	+ 7·6 − 5·6
48	1·79	3	+ 7·4 − 5·4
53	2·19	3	+ 7·3 − 5·3
58	2·55	0·5	+ 7·2 − 5·2
68	3·22	1·5	+ 7·2 − 5·2
78	3·61	1·5	+ 7·2 − 5·2
88	3·88	2·0	+ 7·1 − 5·1
98	4·06	1·0	+ 7·1 − 5·1
108	4·29	1·5	+ 7·1 − 5·1
123	4·37	1·0	+ 7·1 − 5·1
148	4·38	1·0	+ 7·1 − 5·1
173	4·32	1·0	+ 7·1 − 5·1
198	4·11	1·5	+ 7·1 − 5·1
248	3·98	1·0	+ 7·1 − 5·1
298	3·65	2·0	+ 7·1 − 5·1
348	3·52	1·0	+ 7·1 − 5·1
398	3·24	1·0	+ 7·1 − 5·1
448	3·18	1·0	+ 7·1 − 5·1
498	3·02	1·0	+ 7·1 − 5·1
598	2·67	1·5	+ 7·1 − 5·1
698	2·39	1·0	+ 7·1 − 5·1
798	2·24	1·5	+ 7·1 − 5·1
898	2·06	2·0	+ 7·1 − 5·1
997	1·87	2·0	+ 7·1 − 5·1

† ±0·5 eV.
‡ 90% confidence limits.
¶ Given in table 2.

the systematic errors. These errors, which arise from uncertainties in the parameters of equation (1), are listed separately in table 2.

Table 2

Possible source of systematic error	Maximum possible systematic error in the cross section		
Measurement of signal (correction for counting system dead time)		±0·5(0·1)	
Calibration of electron multiplier		±2·5(3·0)	
Measurement of I	+1·2(2·2)		−0·2(1·2)
Measurement of J	+1·25		−0·25
Measurement of V		±0·15	
Measurement of v		0	
Measurement of h		±0·4	
Measurement of F		±0·5	
Uncertainty of angle of beam intersection	+0		−0·5
$E^{-1/2}$ correction term		±0·3†(2·0‡)	
Contributions to I from extraneous ions¶ in the parent beam	+0·5(2·0)		−0

Where the errors for O^{2+} differ from those for O^+, the former are given in brackets.
† At 50 eV and ‡ at 80 eV, errors decrease at higher energies and increase at lower.
¶ O_2^{2+} ions in the O^+ beam; O^+ ions in the O^{2+} beam.

The theoretical cross sections of Thomas and Garcia (1969), of Lotz (1968) and of Moores are plotted in figure 4 for comparison. All these calculations refer only to the ground state of O^+ but all take account of inner shell ionization. At energies up to the peak, the classical and Coulomb–Born cross sections considerably exceed the measured data. However, at higher energies, the inadequacy of the classical E^{-1} energy dependence becomes apparent whereas the Coulomb-Born approximation approaches the measured values. It is of interest to note the remarkable agreement of the relatively simple semiempirical calculations of Lotz.

At high incident energies the Bethe approximation is valid and ionization cross sections should exhibit an energy dependence given by,

$$Q = \frac{A \lg cE}{E} + \frac{B}{E}$$

where A, B and c are constants for a given ion or atom. The present experiment does not extend into the Bethe regime, nevertheless at lower energies there is a regime in which a simple empirical relationship appears to be generally valid, namely

$$Q = \frac{\alpha}{E} \lg \frac{E}{\beta}.$$

Here α and β are also constants for particular ions. In the case of O^+, this energy regime extends from 100 eV to the limit of the experiment at 1 keV and is clearly shown in figure 5 where QE is plotted against $\lg E$. The cross section determined

from the slope of this plot is

$$Q = \frac{1530}{E} \lg \frac{E}{55{\cdot}0} (10^{-17}\ \mathrm{cm}^2) \tag{5}$$

where E is in units of electron volts.

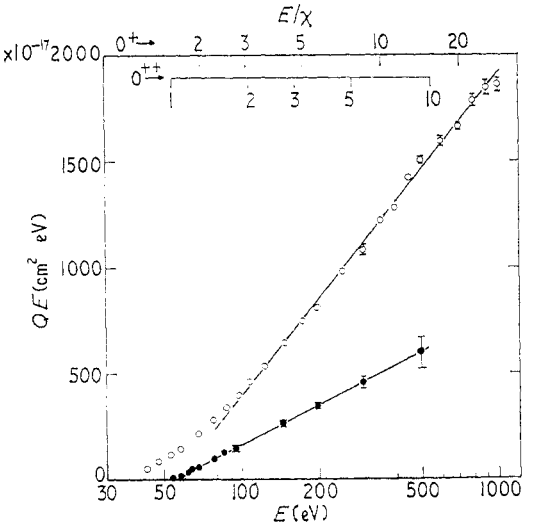

Figure 5. The product (QE) of the measured cross section Q and the incident electron energy E plotted against lg E. Error bars represent 90% confidence limits where these exceed the point diameters. Results for O^+ are shown by open circles and the linear relationship above 100 eV is expressed by equation (5). Results for O^{2+} are shown by solid circles and the linear relationship is expressed by equation (6).

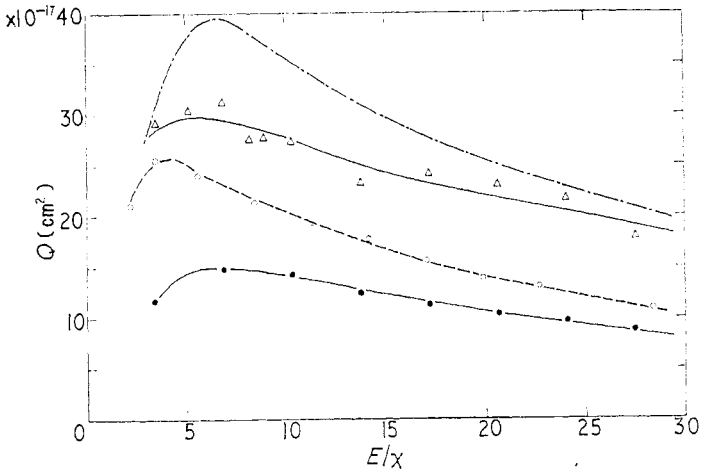

Figure 6. The ionization cross section for atomic nitrogen as a function of incident electron energy in units of the ionization potential χ. Solid circles show the result of Smith *et al.* (1962), open triangles the results of Peterson (1964) and the broken line curve the Born and Ochkur approximation of Peach (1970). The dashed curve drawn through the open circle data points shows the present experimental result for O^+ normalized by the factor $(\chi_{O^+}/\chi_N)^2$.

O^+ is isoelectronic with atomic nitrogen and a comparison of its normalized cross section $Q(E)(\chi_{O^+}/\chi_N)^2$ with the cross section for nitrogen can be of value in resolving ambiguities in the latter. In figure 6, ionization cross sections of N are plotted against E/χ. Two experimental results are shown, the first being obtained using the crossed electron–thermal energy atom beam technique by Smith *et al.* (1962) and the second using a crossed electron–fast atom beam technique by Peterson (1964). The theoretical curve of Peach (1970) was obtained using the Born and Ochkur approximations and agrees more closely with Peterson's results. The normalized cross section of O^+ lies below these two but above the results of Smith *et al.* It is to be expected that the action of the ionic Coulomb field will cause the normalized cross section to lie above that of the isoelectronic atom except at higher energies where agreement between the ion and the thermal atom beam data is improving. It can be concluded that the present results support those of Smith *et al.*, which is not entirely unexpected in view of the experimental problems associated with a fast atom beam technique.

B. $O^{2+} + e \rightarrow O^{3+} + 2e$

6. Apparatus

The anode of the source was run at 200 V and the parent O^{2+} ions were extracted by a potential difference of 10 kV, the instantaneous pulsed beam current was typically $2{\cdot}5 \times 10^{-9}$ A. The maximum signal of O^{3+} was 70 counts s^{-1} superimposed upon a background of charge stripped O^{3+} ions amounting to about 300 counts s^{-1}. Due to limitations in the time for data acquisition, the statistical errors in the present experiment are greater than for those reported for O^+ and an assumption was made that the efficiency of detection of O^{3+} ions was the same as that for N^{3+} ions with equal energy (see Aitken *et al.* 1971).

7. Results and discussion

The measured cross section is shown plotted against incident electron energy in figure 7. It has been corrected (using an $E^{-1/2}$ term) for a small negative signal

Table 3. Electron impact ionization cross section O^{2+} to O^{3+}

Mean incident electron energy (eV)†	Measured cross section (10^{-17} cm^2)	Random error (± %)‡	Maximum systematic error (%)¶
54·2	0·091	95	+43 −40
58·2	0·277	42	+19·9 −17·4
62·2	0·502	22	+15·1 −12·6
64·2	0·772	11	+12·9 −10·4
68·2	0·820	15	+12·8 −10·3
78·2	1·21	9	+11·6 − 8·1
85·2	1·50	5	+11·2 − 7·7
95·2	1·55	7	+11·1 − 7·6
145·2	1·83	5	+10·6 − 7·1
198·2	1·73	4	+10·5 − 7·0
298·2	1·54	6	+10·5 − 7·0
498·2	1·21	15	+10·4 − 6·9

† ±0·5 eV.
‡ 90% confidence limits.
¶ Given in table 2.

observed below the ionization threshold; the correction is less than 5% at the peak value of the measured cross section. Numerical values are listed in table 3, together with random and maximum systematic errors, the latter arising from the individual parameters given in table 2.

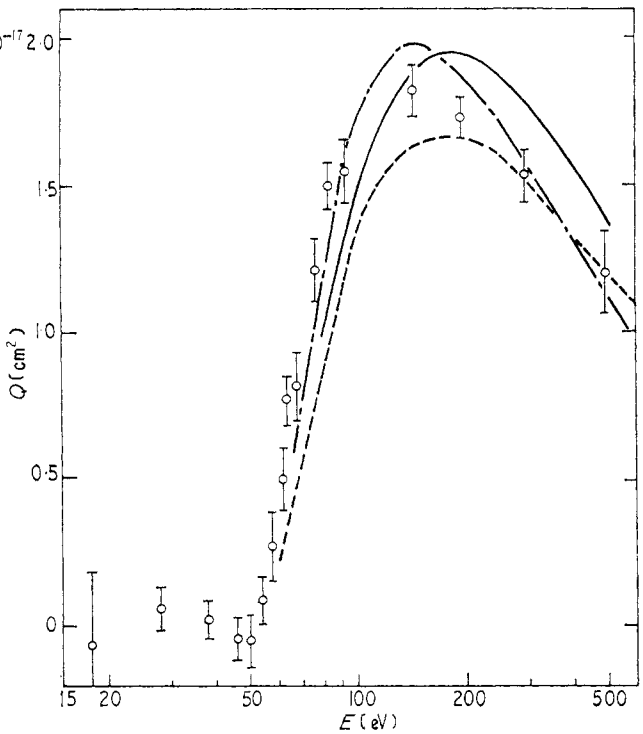

Figure 7. The measured ionization cross section by electron impact for O^{2+}. The curves are as described in figure 4.

Examination of the cross section using an expanded energy scale yields evidence of ionization below the ^3P ground state threshold at 54·9 eV. Redhead (1969) has observed ionization from both the ^1S and ^1D states whose lifetime (Bates 1960) are 0·55 s and 36 s respectively. The ionization channels likely to contribute to the measured cross section are:

Outer shell ionization

$$O^{2+}(1s^22s^22p^2)\text{—}\begin{bmatrix} ^1S\text{—}(49{\cdot}6\text{ eV}) \\ ^1D\text{—}(52{\cdot}4)\text{ eV} \\ ^3P\text{—}(54{\cdot}9\text{ eV}) \end{bmatrix} \rightarrow O^{3+}(1s^22s^22p)$$

Inner shell ionization

$$O^{2+}(1s^22s^22p^2)\text{—}\begin{bmatrix} ^1S\text{—}(58{\cdot}4\text{ eV}) \\ ^1D\text{—}(61{\cdot}3\text{ eV}) \\ ^3P\text{—}(63{\cdot}8\text{ eV}) \end{bmatrix} \rightarrow O^{3+}(1s^22s2p^2)$$

As in the case of O^+ an estimate was made of the metastable concentration from the relative slopes of the measured cross section near to the metastable and ground state thresholds. The present experiment does not resolve between ionization contributions from the individual ^1S and ^1D states but their combined signal indicates that their fractional concentration in the parent beam is $30 \pm 10\%$. Therefore, on the basis of the Lotz formulation, the measured cross section is likely to overestimate the ground state cross section by $(7{\cdot}5 \pm 2{\cdot}5)\%$ at 100 eV, $(4{\cdot}5 \pm 1{\cdot}5)\%$ at 200 eV and less at higher energies. Specific contributions from inner shell ionization cannot be distinguished but are taken into account in the three theoretical cross sections shown in figure 7 which are generally in better agreement at the peak cross section than in the case of O^+.

The present results plotted in the form QE against $\lg E$ are shown in figure 5. Despite rather large error bars, which represent 90% confidence limits on each point, a linear relationship exists over almost the entire energy range of the experiment, so that the cross section can be represented by the equation:

$$Q = \frac{626}{E} \lg \frac{E}{55{\cdot}0} (10^{-17}\ \text{cm}^2) \tag{6}$$

where E is the incident electron energy.

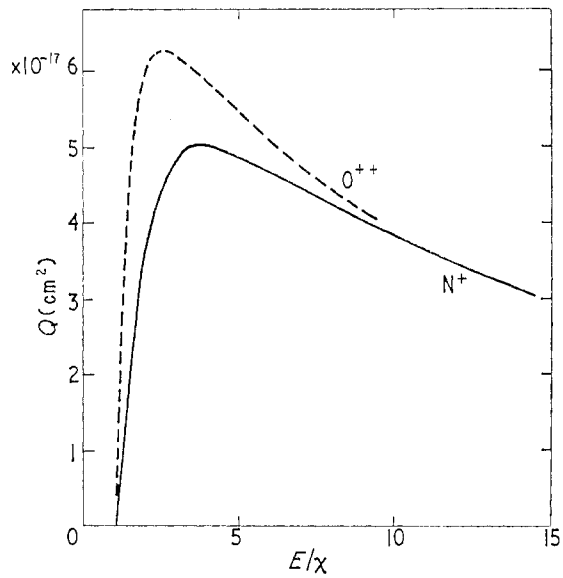

Figure 8. The ionization cross section of O^{2+} normalized to that of N^+ according to the ratio $(\chi_{O^{2+}}/\chi_{N^+})^2$.

The O^{2+} ion is isoelectronic with N^+ and its normalized cross section $Q(\chi_{O^{2+}}/\chi_{N^+})^2$ is shown in figure 8 together with the N^+ results of Harrison *et al.* (1963). The normalized cross sections tend to the same value at the highest experimental energy ($E/\chi \simeq 10$), but at lower energies the O^{2+} results are larger and are compatible with the effect of the greater Coulomb field.

Acknowledgments

The authors wish to thank Dr D. L. Moores for communicating his unpublished work with permission to display it here. In addition we are also indebted to Dr A. J. Dixon for his contribution to the data acquisition on O^{2+}. We also wish to acknowledge the skilled assistance of G. H. Hirst and P. R. White in the maintenance and modification of the apparatus.

References

AITKEN, K. L., HARRISON, M. F. A., and RUNDEL, R. D., 1971, Part 2 of this paper.

BATES, D. R., 1960, *Physics of the upper atmosphere*, Ed. J. A. Radcliffe (New York, London: Academic Press), p.302.

DALY, N. R., and POWELL, R. E., 1967, *Proc. Phys. Soc.*, **90,** 629–35.

DANCE, D. F., HARRISON, M. F. A., RUNDEL, R. D., and SMITH, A. C. H., 1967a, *Proc. Phys. Soc.*, **92,** 577–88.

DANCE, D. F., HARRISON, M. F. A., and RUNDEL, R. D., 1967b, *Proc. R. Soc.* A, **299,** 525–37.

DORMAN, F. H., and MORRISON, J. D., 1963, *J. chem. Phys.*, **39,** 1906–7.

HARRISON, M. F. A., DOLDER, K. T., and THONEMANN, P. C., 1963, *Proc. Phys. Soc.*, **82,** 368–71.

HARRISON, M. F. A., 1968, *Methods of experimental physics.*, Vol. 7A, Eds B. Bederson and W. L. Fite (New York: Academic Press), p. 111.

LOTZ, W., 1968, *Z. Phys.*, **216,** 241–7.

PEACH, G., 1970, *J. Phys.* B: *Atom. molec. Phys.*, **3,** 328–49.

PETERSON, J. R., 1964, *Atomic collision processes*, Ed. M. R. C. McDowell (Amsterdam: North Holland) pp. 465–73.

REDHEAD, P. A., 1969, *Can. J. Phys.*, **47,** 2449–57.

SMITH, A. C. H., CAPLINGER, E., NEYNABER, R. H., and TRUJILLO, S. M., 1962, *Phys. Rev.*, **127,** 1647–9.

THOMAS, B. K., and GARCIA, J. D., 1969, *Phys. Rev.*, **179,** 94–101.

TURNER, B. R., RUTHERFORD, J. A., and COMPTON, D. M. J., 1968, *J. chem. Phys.*, **48,** 1602–8.